

Method for Solving Chance Constrained Optimal Control Problems Using Biased Kernel Density Estimators

Rachel E. Keil*
 Alexander T. Miller[†]
 Mrinal Kumar[‡]
 Anil V. Rao[§]

Abstract

A method is developed to numerically solve chance constrained optimal control problems. The chance constraints are reformulated as nonlinear constraints that retain the probability properties of the original constraint. The reformulation transforms the chance constrained optimal control problem into a deterministic optimal control problem that can be solved numerically. The new method developed in this paper approximates the chance constraints using Markov Chain Monte Carlo (MCMC) sampling and kernel density estimators whose kernels have integral functions that bound the indicator function. The nonlinear constraints resulting from the application of kernel density estimators are designed with bounds that do not violate the bounds of the original chance constraint. The method is tested on a non-trivial chance constrained modification of a soft lunar landing optimal control problem and the results are compared with results obtained using a conservative deterministic formulation of the optimal control problem. The results show that this new method efficiently solves chance constrained optimal control problems.

*Ph.D. Candidate, Department of Mechanical and Aerospace Engineering, University of Florida, Gainesville, FL 32611-6250. E-mail: rekeil@ufl.edu

[†]Ph.D. Candidate, Department of Mechanical and Aerospace Engineering, University of Florida, Gainesville, FL 32611-6250. E-mail: alexandertmiller@ufl.edu

[‡]Associate Professor, Department of Mechanical and Aerospace Engineering, The Ohio State University, Columbus, OH 43210. AIAA Senior Member. E-mail: kumar.672@osu.edu

[§]Professor, Erich Farber Faculty Fellow and University Term Professor, Department of Mechanical and Aerospace Engineering, University of Florida, Gainesville, FL 32611-6250. E-mail: anilvrao@ufl.edu. Corresponding Author.

1 Introduction

Optimal control problems arise frequently in different fields including various branches of engineering and disciplines outside of engineering. The goal of solving an optimal control problem is to determine the state and control of a controlled dynamic system that optimizes a performance index subject to dynamic constraints, path constraints and boundary conditions [1]. The applications for optimal control problems include robotics, disease control, chemical processes, and flight. Optimal control problems can be broadly categorized as either deterministic or stochastic. In a deterministic optimal control problem, no part of the optimal control problem contains uncertainty. By contrast, in a stochastic optimal control problem uncertainty can be present in any part of the optimal control problem. Uncertainty in an optimal control problem arises in various forms including process noise, measurement noise, and uncertainty in the constraints. When such uncertainty is present in the constraints of the stochastic optimal control problem, these optimal control problems are known as chance constrained optimal control problems (CCOCPs).

Obtaining a solution to a CCOCP analytically is possible only for simple problems. Analytical treatment of chance constraints has been most extensively explored in the domain of robust model predictive control (RMPC), with applications that include traffic control [2], chemical process control [3], and others [4, 5]. Due to the small number of problems solvable analytically, solutions to most CCOCPs must be obtained using numerical methods. Numerically solving a CCOCP is challenging due to the probabilistic formulation of the chance constraints. A simple approach to solving a CCOCP numerically is to reformulate the chance constraints as worst case scenario deterministic constraints. This reformulation transforms the CCOCP to a deterministic optimal control problem. It is noted, however, that this worst case scenario deterministic optimal control problem results in a very conservative solution. Additionally, this deterministic optimal control problem could even prove to be infeasible [6]. The issues with the worst case scenario method are in large part due to not incorporating stochastic properties in the deterministic constraints. As a result, it would be preferable to reformulate the chance constraints as deterministic constraints in an analogous way to how stochastic processes are often reformulated as deterministic processes that incorporate key stochastic properties (for example, the key properties of a Gaussian distribution as used in a Kalman filter). If such a formulation could be obtained for the chance constraints, the CCOCP would be transformed to a numerically solvable deterministic optimal control problem that incorporates key properties of the CCOCP.

Various methods have been developed to transform chance constraints to nonlinear constraints that retain the main stochastic characteristics of the chance constraints [7]. In the method of Ref. [8], weighted summations are used to approximate the chance constraints as deterministic constraints. Next, in the methods of Refs. [9, 10, 11], the chance constraint is transformed using Gaussian properties to a deterministic form. Note, however, that the methods of Refs. [8, 9, 10, 11] are applicable only to linear chance constrained optimization problems. In addition, Ref. [12] transforms the chance constraint to a deterministic form using Gaussian properties. The approach of Ref. [12] can be applied to chance constrained linear quadratic Gaussian problems. In contrast, the method of Ref. [13] uses arbitrary non-Gaussian distributions to determine a deterministic approximation of the chance constraint. It is noted, however, that the method of Ref. [13] is only applicable to linear chance constrained optimization problems. A method applicable to a more general class of chance constrained optimization problems is presented in Ref. [14], which provides various deterministic expressions to approximate a chance constraint based on available information about the chance constraint. The method of Ref. [14] can be difficult to implement depending on the form of the constraint. In Ref. [15], under the assumptions of convex and affine relations for the chance constraint, a convex chance constraint approximation is constructed. As such, the method of Ref. [15] is also applicable only to a specific subset of chance constraints. Another method of interest is the sample average approximation method of Ref. [16]. In the method of Ref. [16], an approximate deterministic constraint is applied using the indicator function, a function form which can increase the numerical difficulty of obtaining a solution. In the method of Ref. [17], linear approximations that depend on the indicator function are employed to effectively transform the chance constrained optimization problem to a deterministic optimization problem. This dependence on the indicator function can increase computational expense in solving this deterministic optimization problem. A method that is more computationally efficient than that of Ref. [17] is the scenario approach of Refs. [18, 19]. The scenario approach determines the worst case scenario objective by using deterministic constraints resulting from the application of a finite number of samples of the uncertainty to the chance constraints. The disadvantage of the scenario approach is that without numerically restrictive fine tuning [20], the resulting solutions are overly-conservative. This conservatism results from the nonlinear constraint approximation being conservative relative to the original chance constraint. As such, more recent methods to transform chance constraints to nonlinear constraints are designed to be less conservative as well

as being applicable to a wider range of chance constraints.

More recently, sampling methods have been developed for transforming chance constraints to not overly-conservative nonlinear constraints. Similar to the scenario approach, these methods employ sampling to approximate the chance constraint. In the method of Refs. [21, 22, 23], samples are applied to obtain an approximate expectation of various different functions that is a nonlinear approximation of the chance constraint which provides an upper bound on the chance constraint. The disadvantage of the method of Refs. [21, 22, 23] is that the resulting nonlinear approximation can still be too conservative relative to the chance constraint. Another class of methods that applies sampling and kernels leads to less conservative nonlinear constraints. In one such method from Ref. [24], kernels are used with the samples in Reproducing Kernel Hilbert Space to approximate the chance constraint. This method can become computationally difficult as the dimensions of the problem grow. Another method applies kernel density estimators (KDEs) to the samples to obtain a nonlinear approximation of the chance constraint [25, 26]. KDEs result in a nonlinear constraint that is not overly-conservative relative to the chance constraint, at the cost of potentially violating the bounds of the chance constraint unlike the method of Refs. [21, 22, 23]. Developing a method that combines the advantages of the method from Refs. [21, 22, 23] and the KDE method from Refs. [25, 26] would be an improvement on previously developed methods.

In this paper, the criteria for a kernel to provide a KDE that does not violate the bounds of the chance constraint is developed using key results from Refs. [21, 22, 23]. This criteria will be used to define a new method to approximate the chance constraints as KDEs that provide an upper bound on the chance constraint, while not being overly-conservative relative to the chance constraint. In particular, the new method transforms chance constraints to deterministic nonlinear constraints. Consequently, the CCOCP is transformed to a deterministic optimal control problem. Numerical methods can then be applied to solve the transformed CCOCP.

Various numerical methods have been developed for solving deterministic optimal control problems. These methods can be categorized broadly as either indirect or direct methods [27]. Indirect methods use the first order optimality conditions to transform the optimal control problem to a Hamiltonian boundary value problem (HBVP) that is then solved. For direct methods the original optimal control problem is directly solved by parameterizing the states and possibly the control. The direct method of Gaussian quadrature

collocation in the form of either Legendre-Gauss (LG) [28, 29], Legendre-Gauss-Lobatto (LGL) [30] or Legendre-Gauss-Radau (LGR) [31, 32, 33] collocation has broad applicability, in addition to providing high accuracy solutions with exponential convergence [34, 35]. Direct collocation can also be easily paired with readily available software [36, 37]. As a result of the advantages of direct Gaussian quadrature collocation, in this paper LGR collocation will be applied with the new method for transforming chance constraints to deterministic nonlinear constraints to develop a computational framework for efficiently solving CCOCPs in their transformed deterministic form.

The paper is organized as follows. Section 2 gives a brief overview of methods applied to transform chance constraints to nonlinear constraints and uses aspects of these methods to develop the new method. Section 3 describes a general chance constrained optimal control problem. Section 4 provides a brief overview of the LGR collocation method. Section 5 describes the computational framework to numerically solve the transformed CCOCP using available optimal control software. In Section 6, this computational framework is applied to an example. Section 7 provides some conclusions.

2 Chance Constrained Optimization

In this section, a new method is developed for reformulating a chance constrained optimization problem as a deterministic optimization problem. The reformulation is accomplished by transforming the chance constraints to nonlinear constraints that retain key stochastic properties of the chance constraints. The new method developed combines two previously developed methods, and these two methods are described in Section 2.1. The first of the methods, Method 1 described in Section 2.1.1, defines a nonlinear approximation of the chance constraint. This approximation is an approximation of the cumulative distribution function (CDF) of the random variable associated with the chance constraint. The advantage of Method 1 is that the approximation is an upper bound on the chance constraint. The disadvantage of Method 1 is that this approximation of the CDF is allowed to exceed unity. The second of the methods, Method 2 described in Section 2.1.2, uses Kernel Density Estimators (KDE)s to obtain a nonlinear approximation of the chance constraint. The advantages of Method 2 are that the approximation of the CDF stemming from the KDE does not exceed unity and that there is a wide range of functions that can be used for a KDE. The disadvantage

of Method 2 is that the approximation may violate the bound on the chance constraint. Consequently, a new method that combines the advantages of these previously developed methods would be an improvement on said methods.

One particular nonlinear approximation used for Method 1 is the Split-Bernstein approximation described in Ref. [22]. This nonlinear approximation is shown in Section 2.2 to be a KDE with the appropriate choice of parameters. The Split-Bernstein approximation with certain parameters combines the advantage of Method 1 in upper bounding the chance constraint with one of the advantages of Method 2 in having an approximation of the CDF that does not exceed unity. As a result of this last fact, in Section 2.3 the Split-Bernstein KDE is analyzed to determine the necessary criteria for other KDEs to retain these advantages. In the new method, a nonlinear approximation to the chance constraint is defined that applies this necessary criteria in order to use KDEs that ensure an upper bound the chance constraint. This new method is then applied to chance constrained optimal control, as described in Section 3.

2.1 Previous Methods for Reformulating Chance Constraints

To begin the development of the new method, consider the following general chance constrained optimization problem:

$$\begin{aligned} \min_{z \in Z} J(z) \\ P(\mathbf{F}(\mathbf{z}, \boldsymbol{\xi}) \geq \mathbf{q}) \geq 1 - \epsilon, \end{aligned} \tag{1}$$

where \mathbf{z} is a decision variable defined on the feasible set $\mathbf{Z} \subset \mathbb{R}^n$ and $\boldsymbol{\xi}$ is a random variable with a probability density function (PDF) $f_{\boldsymbol{\xi}}(\boldsymbol{\xi})$ supported on set $\Omega \subseteq \mathbb{R}^d$ for which samples of $\boldsymbol{\xi}$ will be used. The function $\mathbf{F}(\mathbf{z}, \boldsymbol{\xi}) \geq \mathbf{q}$ is an event in the probability space $P(\cdot)$, where $\mathbf{F}(\cdot)$ maps $\mathbb{R}^n \times \mathbb{R}^d \rightarrow \mathbb{R}^{n_g}$ and ϵ is the risk violation parameter. The function $\mathbf{F}(\mathbf{z}, \boldsymbol{\xi})$ is itself a random variable $\boldsymbol{\psi}$ whose associated probabilistic properties such as its PDF are assumed to be unknown. Consequently, the constraint of Eq. (1) can be redefined as

$$P(\boldsymbol{\psi} \geq \mathbf{q}) \geq 1 - \epsilon, \tag{2}$$

or, equivalently

$$P(\boldsymbol{\psi} < \mathbf{q}) \leq \epsilon. \tag{3}$$

Because the event $\psi < \mathbf{q}$ is a vector, Eq. (2) or (3) is a joint chance constraint. Using Boole's inequality together with the approach of Refs. [9] and [22], the chance constraint given in Eq. (2) can be redefined in terms of the following two conservative constraints (see Refs. [9] and [22] for the proof):

$$\begin{aligned} P(\psi \geq q_m) &\geq 1 - \epsilon_m, \\ \sum_{m=1}^{n_g} \epsilon_m &\leq \epsilon, \end{aligned} \tag{4}$$

where $m \in [1, \dots, n_g]$ is the index corresponding to the m th component of the event. It should be noted that in Ref. [15] the first of the two scalar constraints in Eq. (4) was also applied, but not the second as this constraint would destroy the convexity of the problem. As the retention of convexity is not required for application of numerical methods, both constraints can be used to replace the chance constraint of Eq. (2).

2.1.1 Method 1: Nonlinear Approximation of the Chance Constraint

In the first method, an upper bound on the chance constraint is defined as the expectation of some function $w(\xi)$. Because the expectation cannot be obtained analytically, a nonlinear approximation of the expectation is obtained using sampling. In particular, samples of ξ are obtained using Markov Chain Monte Carlo (MCMC) sampling or by some simpler method when advantageous properties of ξ are assumed. Formally, the upper bound on the chance constraint given in Eq. (4) for the first method is defined in terms of the expectation \mathbb{E} and the indicator function $1_{(\cdot)}$ as:

$$1 - \epsilon_m \leq P(\psi \geq q_m) = \mathbb{E}_{\xi}[1_{[q_m, +\infty)}(\psi - q_m)] \leq \mathbb{E}_{\xi}[w(\psi - q_m)], \tag{5}$$

where $w(\cdot)$ represents a function that has the property

$$1_{[q_m, +\infty)}(\psi - q_m) \leq w(\psi - q_m), \quad \forall (\psi - q_m). \tag{6}$$

Different nonlinear approximations of the upper bound on the chance constraint from Eq. (5) were developed in Refs. [21, 22, 23]. The property of the function $w(\cdot)$ in Eq. (6) and the type of samples obtained for ξ are what ensure that the nonlinear approximation of the expectation still provides an upper bound on the chance constraint. The function $w(\cdot)$, however, has the disadvantage of being allowed to pass unity instead of being bounded by it. As a result, the nonlinear approximation of the chance constraint of Eq. (5) resulting from Method 1 will exceed unity and so cannot be an approximate CDF. Consequently, in the next section

a second method that uses KDEs to obtain a nonlinear approximation of the chance constraint which is an approximate CDF is considered.

2.1.2 Method 2: Kernel Density Estimator

The second method, described in Ref. [26], uses KDEs to obtain a nonlinear approximation of the chance constraint. The nonlinear approximation is obtained by first applying kernels to determine an approximate PDF \hat{f}_ψ of a desired random variable ψ , using samples ψ_j of the random variable. The approximate PDF is defined as follows:

$$\hat{f}_\psi(q_m) = \frac{1}{N} \sum_{j=1}^N \frac{1}{h} k(\eta_j), \quad (7)$$

where $k(\cdot)$ is the kernel, h is the bandwidth, $j = 1, \dots, N$ is the number of samples and η_j is defined as

$$\eta_j = \frac{q_m - \psi_j}{h}. \quad (8)$$

The right hand side of Eq. (7) is the KDE. To define the relation between the chance constraint and the KDE, first the approximate probability \hat{p} is defined as

$$\hat{p}(\psi < q_m) = \int_{-\infty}^{q_m} \hat{f}_\psi(x) dx. \quad (9)$$

Then, applying the general form of a KDE from Eq. (7) to the right hand side of Eq. (9):

$$\int_{-\infty}^{q_m} \hat{f}_\psi(x) dx = \frac{1}{Nh} \sum_{j=1}^N \int_{-\infty}^{q_m} k\left(\frac{x - \psi_j}{h}\right) dx. \quad (10)$$

Using the definition of η_j from Eq. (8), Eq. (10) can be reformulated as:

$$\frac{1}{Nh} \sum_{j=1}^N \int_{-\infty}^{q_m} k\left(\frac{x - \psi_j}{h}\right) dx = \frac{1}{N} \sum_{j=1}^N \int_{-\infty}^{\eta_j} k(v_j) dv_j. \quad (11)$$

The following integrated function of the kernel can now be defined as:

$$K(\eta_j) = \int_{-\infty}^{\eta_j} k(v_j) dv_j. \quad (12)$$

Using Eq. (12), the approximation of the chance constraint given in Eq. (9) can then be defined relative to a general KDE as

$$\hat{p}(\psi < q_m) = \frac{1}{N} \sum_{j=1}^N K(\eta_j), \quad (13)$$

where the right hand side is the approximate CDF of ψ bounded by q_m . The summation is an approximate CDF as it is dependent on a kernel designed such that $K(\eta)$ is bounded by unity. Finally, using the approximation of Eq. (13), the KDE is related to the chance constraint of Eq. (4) as follows:

$$P(\psi \geq q_m) \approx 1 - \frac{1}{N} \sum_{j=1}^N K(\eta_j). \quad (14)$$

Comparing Eq. (14) to Eq. (5), the approximate chance constraint resulting from Method 2 does not bound the original chance constraint like the approximation from Method 1. As a result, the disadvantage of Method 2 is that the approximate chance constraint resulting from the application of KDEs can lie outside the boundary of the original chance constraint.

2.1.3 Comparison of the Two Methods

When comparing the two methods described in Sections 2.1.1 and 2.1.2, the method of Section 2.1.1 has the advantage of placing an upper bound on the chance constraint. The functions used in this method have the requirement of Eq. (6), leading to an approximation of the CDF of ψ that is not bounded by unity. It is noted, however, that KDEs are designed with functions that lead to an approximate CDF. Combining this last fact with the wide variety of kernels that can be applied to a given problem, makes the method of Section 2.1.2 an attractive option for approximating a chance constraint. The main issue with the method of Section 2.1.2 is the possibility of violating the bounds on the chance constraint. The new method is an improvement on the methods of Sections 2.1.1 and 2.1.2 as it utilizes the necessary underlying functional form to ensure the upper bound on the chance constraint from the method of Section 2.1.1, while retaining the versatility and other characteristics of KDEs. In the new method, MCMC samples of ξ are used with KDEs that satisfy the necessary requirements to obtain a new nonlinear approximation of the chance constraint that upper bounds the chance constraint. A nonlinear approximation stemming from Method 1 that both upper bounds the chance constraint and with the right choice of parameters is also a KDE is the Split-Bernstein approximation. Consequently, to determine the necessary requirements for a KDE to upper bound the chance constraint, the Split-Bernstein approximation will be studied.

2.2 Split-Bernstein Approximation

In this section, the Split-Bernstein approximation and its KDE form are presented to define the necessary criteria for a KDE to upper bound the chance constraint. The Split-Bernstein approximation from Ref. [22] follows from the inequality of Eq. (5) as:

$$1 - \epsilon_m \leq \mathbb{E}_{\boldsymbol{\xi}}[1_{[q_m, +\infty)}(\alpha(\psi - q_m))] \leq \mathbb{E}_{\boldsymbol{\xi}}[\Xi_{\alpha}(\alpha(\psi - q_m))], \quad \forall \alpha > 0, \quad (15)$$

where the function $w(\cdot)$ from Eq. (5) is replaced by the following Split-Bernstein function Ξ_{α} :

$$\Xi_{\alpha}(\alpha(\psi - q_m)) = \begin{cases} \exp(\alpha_+(\psi - q_m)), & \text{if } \psi - q_m \geq 0, \\ \exp(\alpha_-(\psi - q_m)), & \text{if } \psi - q_m < 0. \end{cases} \quad (16)$$

Both α_+ and α_- are parameters defined such that the piecewise function of Eq. (16) converges to the indicator function when $\alpha_+ \rightarrow 0$ and $\alpha_- \rightarrow +\infty$ (Proof provided in Ref. [22]). This convergence can be seen in Fig. 1 where $\psi \geq x$ is an event with bound $x = 0$ and $F(x)$ represents the Split-Bernstein function.

The Split-Bernstein upper bound on the constraint from Eq. (15) requires evaluation of the expectation, where computing the expectation requires integration of the unknown PDF of ψ . Samples of $\psi(\boldsymbol{\xi})$ are available as a function of the MCMC samples of $\boldsymbol{\xi}$. Based on the samples of $\boldsymbol{\xi}$, an expression that converges to the expectation $\mathbb{E}_{\boldsymbol{\xi}}[\Xi_{\alpha}(\cdot)]$ of Eq. (15) was developed in Ref. [22] and those portions of the result obtained in Ref. [22] that are relevant are presented as **Lemma 1** shown below.

Lemma 1. Assume the following:

1. $\mathbb{E}_{\boldsymbol{\xi}}[\Xi_{\alpha}(\alpha(q_m - F(\mathbf{z}, \boldsymbol{\xi}))) \leq \epsilon_m]$ is a nonempty convex set $\mathbf{x} \in \mathbf{X}_{\Xi}$.
2. $\mathbb{E}_{\boldsymbol{\xi}}[\Xi_{\alpha}(\alpha(q_m - F(\mathbf{z}, \boldsymbol{\xi})))]$ exists for $\mathbf{x} \in \mathbf{X}_{\Xi}$.
3. The moment-generating function $\Xi_{\alpha}(\alpha(q_m - F(\mathbf{z}, \boldsymbol{\xi}))) - \mathbb{E}_{\boldsymbol{\xi}}[\Xi_{\alpha}(\alpha(q_m - F(\mathbf{z}, \boldsymbol{\xi})))], \forall \mathbf{z} \in \mathbf{Z}_{\Xi}$ exists in a neighborhood of zero.
4. For any $\boldsymbol{\xi} \in \Omega$ there exists a positive real-valued function $\phi(\boldsymbol{\xi})$ for which the expectation $\mathbb{E}[\phi(\boldsymbol{\xi})] = \Phi(\cdot)$ also exists such that, for any $\mathbf{z}_1, \mathbf{z}_2 \in \mathbf{X}_{\Xi}$, we have

$$|\Xi_{\alpha}(\alpha(q_m - F(\mathbf{z}_1, \boldsymbol{\xi}))) - \Xi_{\alpha}(\alpha(q_m - F(\mathbf{z}_2, \boldsymbol{\xi})))| \leq \phi(\boldsymbol{\xi}) \|\mathbf{z}_1 - \mathbf{z}_2\|. \quad (17)$$

5. The moment-generating function of $\phi(\boldsymbol{\xi})$ exists in a neighborhood of zero.

Under Assumptions 1-5 above, the expression

$$\frac{1}{N} \sum_{j \in J_+} \exp(\alpha_+(q_m - F(\mathbf{z}, \xi_j))) + \frac{1}{N} \sum_{j \in J_-} \exp(\alpha_- F(\mathbf{z}, \xi_j)) \quad (18)$$

converges to the expectation

$$\mathbb{E}_{\boldsymbol{\xi}}[\Xi_{\alpha}(\alpha(q_m - F(\mathbf{z}, \boldsymbol{\xi})))] \quad (19)$$

for a large enough number of MCMC samples ξ_j for $j = 1, \dots, N$.

Proof of Lemma 1. Proof provided in the Appendix of Ref. [22]. □

As a result of **Lemma 1**, the Split-Bernstein expectation of Eq. (15) can be approximated as:

$$\frac{1}{N} \sum_{j \in J_+} \exp(\alpha_+(q_m - \psi_j)) + \frac{1}{N} \sum_{j \in J_-} \exp(\alpha_-(q_m - \psi_j)) \leq \epsilon_m. \quad (20)$$

For the summation of Eq. (20), the event $\psi < q_m$ is indexed as $J_+ \in (q_m - \psi_j > 0)$ and $J_- \in (q_m - \psi_j \leq 0)$.

The summation on the left hand side of Eq. (20) is the Split-Bernstein approximation.

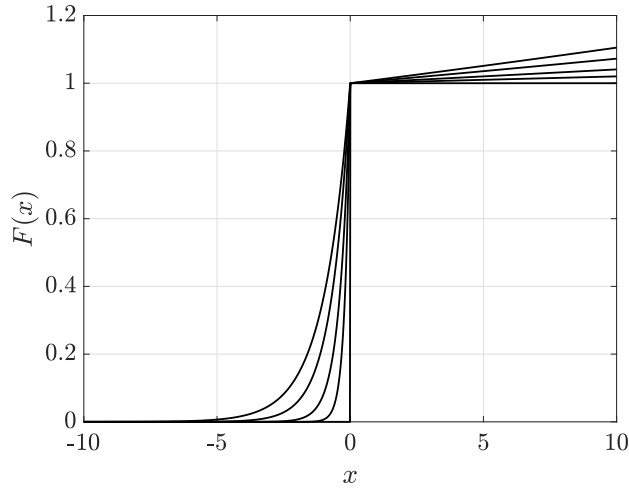


Figure 1: Convergence of the Split-Bernstein function as $\alpha_+ \rightarrow 0$ and $\alpha_- \rightarrow +\infty$.

2.2.1 Split-Bernstein Approximation as a KDE

The Split-Bernstein approximation in Eq. (20) assigns a number that can be greater than unity for samples of ψ in $J_+ \in (q_m - \psi_j > 0)$. As such, the Split-Bernstein approximation is not an approximate CDF in its

general form. KDEs employ kernels that are bounded by unity, thus ensuring that the right hand side of Eq. (13) derived from the general form of a KDE is an approximate CDF. Choosing $\alpha_+ = 0$ and $\alpha_- = \alpha$ for the Split-Bernstein approximation ensures that the approximation cannot exceed unity. Therefore, Eq. (20) can be formulated as the following approximate CDF:

$$\frac{1}{N} \sum_{j \in J_+} 1 + \frac{1}{N} \sum_{j \in J_-} \exp(\alpha(q_m - \psi_j)) \leq \epsilon_m, \quad (21)$$

where the left-hand side of Eq. (21) is the Split-Bernstein approximate CDF. Consequently, taking the derivative of the left hand side of Eq. (21) leads to the following approximate PDF of ψ :

$$\hat{f}_\psi(q_m) = \frac{1}{N} \sum_{j \in J_+} 0 + \frac{1}{N} \sum_{j \in J_-} \alpha \exp(\alpha(q_m - \psi_j)). \quad (22)$$

Suppose now that α is defined as

$$\alpha = \frac{1}{h}. \quad (23)$$

Using α from Eq. (23), Eq. (22) transforms to the form of Eq. (7), indicating that the Split-Bernstein approximation is a potential KDE. The associated candidate kernel $k_{SB}(\cdot)$ from Eq. (22) for the Split-Bernstein approximation is

$$k_{SB}(\eta) = \begin{cases} 0, & \eta > 0 \\ \exp(\eta), & \eta \leq 0. \end{cases} \quad (24)$$

The inequality cases of Eq. (24) replace the inequalities of Eq. (16) by taking

$$\eta > 0 \Rightarrow \frac{q_m - \psi}{h} > 0 \Rightarrow q_m - \psi > 0. \quad (25)$$

It remains to show that the Split-Bernstein candidate kernel satisfies the requirements of a kernel. The requirements of a kernel vary in the literature [38, 39], so three main criteria were chosen by the authors as they encompass the most common requirements. These criteria lead to the following proposition.

Proposition 1. The Split-Bernstein approximation with $\alpha_+ = 0$ leads to the kernel of Eq. (24) that satisfies the following criteria:

1. $k(\eta) \geq 0$,
2. $\int_{-\infty}^{+\infty} k(x)dx = 1$,

$$3. 0 < \int_{-\infty}^{+\infty} x^2 k(x) dx < +\infty.$$

Proof of Proposition 1. For Case (1), the Split-Bernstein candidate kernel is zero for $\eta > 0$ and always greater than zero for $\eta \leq 0$. Showing that Case (2) is satisfied is straightforward:

$$\int_{-\infty}^{+\infty} k_{SB}(x) dx \Rightarrow \int_{-\infty}^0 \exp(x) dx + \int_0^{+\infty} 0 dx \Rightarrow \exp(x) \Big|_{-\infty}^0 + 0 = 1. \quad (26)$$

Likewise, Case (3) is proven as:

$$\int_{-\infty}^{+\infty} x^2 k_{SB}(x) dx \Rightarrow \int_{-\infty}^0 x^2 \exp(x) dx + \int_0^{+\infty} 0 dx = 2. \quad (27)$$

□

The Split-Bernstein candidate kernel k_{SB} is thus shown to be a kernel. As a result of this fact, the Split-Bernstein approximation is a KDE for $\alpha_+ = 0$ and $\alpha_- = \alpha$. Due to the use of MCMC samples and the form of the Split-Bernstein kernel, the Split-Bernstein approximation retains an upper bound on the chance constraint. Thus in Section 2.3, the Split-Bernstein kernel is analyzed to determine the correct criteria for a kernel that, when combined with the use of MCMC samples, ensures that the associated KDE retains the same upper bound on the chance constraint as Method 1 from Section 2.1.1.

2.3 New Method: Biased Kernel Density Estimators

The approximate probability form derived from a KDE is dependent on the choice of kernel $k(\eta)$. A kernel is placed at each sample and the approximate probability is the average of the integrated sum of these kernels evaluated at the weighted sample distance from some bound q_m (see Eq. (14)). Kernels are often designed such that their mean is at the same location as the sample. Having the mean shift to the right or left of the sample is referred to as “biasing” in this paper. As the approximate probability is the result of an average that is a function of the kernel, changing the location of the kernel mean will cause the approximate probability to increase or decrease. Biasing the kernel will be shown in the following section to be one component of reformulating a KDE so that it will provide an upper bound on the chance constraint.

2.3.1 Bias of the Split-Bernstein Kernel

In this section, the Split-Bernstein kernel is studied to determine whether or not it is a biased kernel. Figure 2 shows the Split-Bernstein kernel for a sample centered at zero. It is seen that the Split-Bernstein kernel has

a sail like shape from $-\infty$ to zero, and is zero otherwise. This shape implies that the mean would be shifted to the left of the sample, indicating that the Split-Bernstein kernel is biased. **Proposition 2** states that the Split-Bernstein kernel is a biased kernel, and this proposition is subsequently proven.

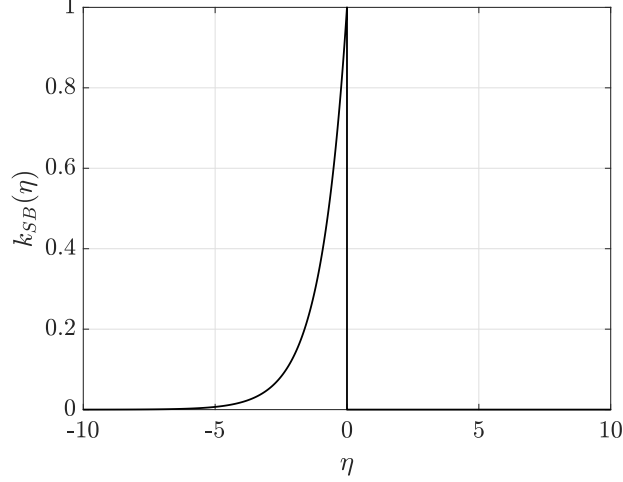


Figure 2: Split-Bernstein kernel.

Proposition 2. The location of the Split-Bernstein kernel mean is $\mu = \psi_j + h \ln(0.5)$, therefore the Split-Bernstein kernel has a bandwidth-dependent bias.

Proof of Proposition 2. The mean is defined to be at a point $w < 0$ where half of the total area under the curve of the kernel lies. It should be noted that the case of $w \geq 0$ is not included as it is trivial to prove such a point does not exist. Then the approximate probability from $-\infty$ to w is

$$\begin{aligned}
\int_{-\infty}^w \exp(x) dx &= \frac{1}{2}, \\
\Rightarrow \exp(x) \Big|_{-\infty}^w &= \frac{1}{2}, \\
\Rightarrow 0 + \exp(w) &= \frac{1}{2}, \\
\Rightarrow w &= \ln\left(\frac{1}{2}\right).
\end{aligned} \tag{28}$$

Because the integral of Eq. (12) was defined using a bound transformation in Eq. (11), the mean μ of the Split-Bernstein kernel can be found from the following relation:

$$w = \ln\left(\frac{1}{2}\right) \Rightarrow \frac{\mu - \psi_j}{h} = \ln\left(\frac{1}{2}\right) \Rightarrow \mu = \psi_j + h \ln\left(\frac{1}{2}\right). \tag{29}$$

Thus the Split-Bernstein kernel mean lies to the left of the sample, proving that this kernel is biased by the bandwidth-dependent amount $h \ln\left(\frac{1}{2}\right)$. \square

In order to demonstrate the importance of the bias resulting from **Proposition 2**, consider adding a positive bias of δ to the Split-Bernstein kernel where

$$0 < \delta \leq |h \ln\left(\frac{1}{2}\right)|, \delta \in \mathbb{R}. \quad (30)$$

The bias δ will result in the following relation for the function $K_{SB}(\cdot)$:

$$K_{SB}(\alpha(\psi - q_m)) = \begin{cases} 1, & \text{if } \psi - q_m \geq \delta, \\ \exp(\alpha(\psi - q_m)), & \text{if } \delta > \psi - q_m \geq 0, \\ \exp(\alpha(\psi - q_m)), & \text{if } \psi - q_m < 0. \end{cases} \quad (31)$$

Recalling from Eq. (6), the Split-Bernstein function has the property:

$$1_{[q_m, +\infty)}(\alpha(\psi - q_m)) \leq \Xi_\alpha(\alpha(\psi - q_m)), \quad \forall \psi. \quad (32)$$

The relation of the Split-Bernstein function to the function $K_{SB}(\cdot)$ when both have a bias of $h \ln\left(\frac{1}{2}\right)$ can be obtained by application of Eqs. (12) and (24) with $\alpha_+ = 0$ and $\alpha_- = \alpha$:

$$1_{[q_m, +\infty)}(\alpha(\psi - q_m)) \leq \Xi_\alpha(\alpha(\psi - q_m)) = K_{SB}(\alpha(\psi - q_m)). \quad (33)$$

For comparison with the formulation of the function $K_{SB}(\cdot)$ in Eq. (31), the indicator function is defined as:

$$1_{[q_m, +\infty)}(\alpha(\psi - q_m)) = \begin{cases} 1, & \text{if } \psi \geq q_m, \\ 0, & \text{if } \psi < q_m. \end{cases} \quad (34)$$

Comparing the function $K_{SB}(\cdot)$ in Eq. (31) with the indicator function in Eq. (34), the inequality of Eq. (33) no longer applies as a portion of the function $K_{SB}(\cdot)$ lies below that of the indicator function. As a result, the conservative bound of Eq. (5) can no longer be guaranteed. Thus a bias of $h \ln\left(\frac{1}{2}\right)$ or smaller is required to ensure that the Split-Bernstein KDE is an upper bound on the chance constraint of Eq. (5). The bias must be bandwidth dependent because the bias should decrease as the function $K_{SB}(\eta)$ converges to the indicator function.

2.3.2 Biased Form of General KDEs

In the previous section it was determined that the bias of the Split-Bernstein kernel, when combined with MCMC sampling, ensures the upper bound on the chance constraint from Eq. (5). This result can be extended to other KDEs that satisfy the requirements of the following **Theorem 1**.

Theorem 1. Suppose there exists a biased kernel $k(\nu)$ defined such that $k(\nu)$ has an integrated function $K(\nu)$ that satisfies the inequality

$$1_{[y, +\infty)} \left(\frac{Y - y}{h} \right) \leq K(\nu), \quad \forall Y, \text{ with } h > 0, \quad (35)$$

$$\nu = \frac{Y - y + B}{h}, \quad B(h) \geq 0, \quad (36)$$

for some event $Y \geq y$ in probability space $P(\cdot)$ where Y is a random variable supported on set $\Omega \subseteq \mathbb{R}^d$ with the bias set as B . If samples of the random variable Y_j are available in a form that ensures **Lemma 1** is satisfied for the function $K(\nu)$, the following inequality holds:

$$\frac{1}{N} \sum_{j=1}^N \int_{-\infty}^{\eta_j + \frac{B}{h}} k(x_j) dx_j \leq P(Y < y) \leq \epsilon_m, \quad (37)$$

where $\epsilon_m \in \mathbb{R}$ and η was defined in Eq. (8).

Proof of Theorem 1. Suppose that a PDF $f_Y(\cdot)$ exists and has bounded first and second moments with a CDF $F_Y(\cdot)$ satisfying:

$$1_{[y, +\infty)} \left(\frac{Y - y}{h} \right) \leq F_Y(\nu), \quad \forall Y, \quad (38)$$

where MCMC samples Y_j of random variable Y are available. Then the sample expectation $\hat{\mathbb{E}}$ is defined as

$$\hat{\mathbb{E}}[F_Y(\nu)] = \frac{1}{N} \sum_{j=1}^N F_Y(\nu_j). \quad (39)$$

Now define the following nonempty compact set:

$$1 - \epsilon_m \leq \mathbb{E}[F_Y(\nu)] \quad (40)$$

where $\mathbb{E}[F_Y(\nu)]$ exists for $h > 0$. Additionally, the expectation as well as the function $F_Y(\cdot)$ satisfy the assumptions of **Lemma 1**. Applying **Lemma 1** to the right hand side of Eq. (39) under the assumption that enough MCMC samples Y_j of the random variable are available, leads to the following relation:

$$1 - \epsilon_m \leq \mathbb{E}[F_Y(\nu)] = \frac{1}{N} \sum_{j=1}^N F_Y(\nu_j). \quad (41)$$

Independent of the result of Eq. (41), it is a known property of probability that

$$P(Y \geq y) = \mathbb{E} [1_{[y, +\infty)}(Y - y)] = \mathbb{E} \left[1_{[y, +\infty)} \left(\frac{Y - y}{h} \right) \right], \quad h > 0, \quad (42)$$

where scaling the indicator function by h does not affect the relation. Additionally, due to the relation of Eq. (38) the following property of probability can be applied to Eq. (42):

$$P(Y \geq y) = \mathbb{E} \left[1_{[y, +\infty)} \left(\frac{Y - y}{h} \right) \right] \leq \mathbb{E}[F_Y(\nu)]. \quad (43)$$

Substituting the relation from Eq. (41) into Eq. (43) leads to the following inequality:

$$1 - \epsilon_m \leq P(Y \geq y) \leq \frac{1}{N} \sum_{j=1}^N F_Y(\nu_j). \quad (44)$$

The form of the PDF $f_Y(\cdot)$ is such that it satisfies the requirements for a kernel from **Proposition 1**.

Therefore

$$F_Y(\nu) = K(\nu). \quad (45)$$

Substituting the relation of Eq. (45) into Eq. (44) leads to the following relation:

$$1 - \epsilon_m \leq P(Y \geq y) \leq \frac{1}{N} \sum_{j=1}^N K(\nu_j). \quad (46)$$

Changing the probability form to its complement in Eq. (46) and substituting η from Eq. (8) leads to the following relation:

$$\frac{1}{N} \sum_{j=1}^N K \left(\eta_j + \frac{B}{h} \right) \leq P(Y < y) \leq \epsilon_m. \quad (47)$$

Applying the relation from Eq. (12) to Eq. (47) results in the following inequality:

$$\frac{1}{N} \sum_{j=1}^N \int_{-\infty}^{\eta_j + \frac{B}{h}} k(x_j) dx_j \leq P(Y < y) \leq \epsilon_m. \quad (48)$$

This concludes the proof. □

Thus the first requirement for a kernel to result in a KDE that provides an upper bound on the chance constraint is that the kernel is biased by a bandwidth dependent amount that is enough to ensure the inequality of Eq. (38). The second requirement is that the sampling method applied ensures convergence of the sample expectation to the expectation that upper bounds the chance constraint from Eq. (5). The new method of biased KDEs applies kernels that satisfy the requirements of **Theorem 1**, as well as MCMC sampling to obtain the nonlinear approximation of the chance constraint from Eq. (37). This nonlinear

approximation provides an upper bound on the chance constraint as well as being an approximate CDF of the random variable, thus retaining the advantages of Methods 1 and 2 from Sections 2.1.1 and 2.1.2, respectively, in a generally applicable manner.

2.4 Biasing the Epanechnikov and Gaussian Kernels

Section 2.3 established the requirement for a kernel to result in a KDE that provides an upper bound on the chance constraint. In this section, this requirement will be applied to the Epanechnikov and Gaussian kernels as these are two common kernels.

2.4.1 Epanechnikov Kernel

The Epanechnikov kernel is considered as it is often referenced as the optimal kernel due to its convergence properties [40]. Letting B represent a bias added to the Epanechnikov kernel from Ref. [41], leads to the following representation of the kernel function K_E :

$$K_E(\eta_j) = \begin{cases} 1, & \text{if } \eta_j \geq 1 - \frac{B}{h_E}, \\ \frac{1}{2} + \frac{3}{4} \left(\eta_j + \frac{B}{h_E} \right) - \frac{1}{4} \left(\eta_j + \frac{B}{h_E} \right)^3, & \text{if } -1 - \frac{B}{h_E} < \eta_j < 1 - \frac{B}{h_E}, \\ 0, & \text{if } \eta_j \leq -1 - \frac{B}{h_E}, \end{cases} \quad (49)$$

where h_E is the bandwidth of the Epanechnikov kernel. Setting B equal to the bandwidth h_E ensures that the kernel function K_E remains greater than or equal to the indicator function everywhere and so satisfies the inequality of Eq. (35).

2.4.2 Gaussian Kernel

The Gaussian kernel is a popular kernel as it is completely smooth and is fairly straightforward to implement numerically. The design of the Gaussian kernel is

$$K_G(\eta_j) = \frac{1}{2} \left(1 + \operatorname{erf} \left(\frac{h_G \eta_j + B}{h_G \sqrt{2}} \right) \right), \quad \forall \eta_j, \quad (50)$$

where h_G is both the bandwidth and the standard deviation and B represents the added bias. Solving for the bias that will result in $K_G = 1$:

$$K_G(\eta_j) = 1 \Rightarrow \operatorname{erf} \left(\frac{h_G \eta_j + B}{h_G \sqrt{2}} \right) = 1 \Rightarrow \frac{h_G \eta_j + B}{h_G \sqrt{2}} = \operatorname{erf}^{-1}(1) \Rightarrow B = \infty. \quad (51)$$

As a result, the Gaussian kernel cannot be biased enough to ensure the inequality of Eq. (35). It is possible to ensure that at least 99% of the Gaussian kernel function K_G satisfies the requirement of Eq. (35) by assigning a bias of $3h_G$. Even though the Gaussian kernel does not satisfy the requirements of **Theorem 1**, it could still provide a useful comparison to other less smooth kernels in numerical application. The three kernel functions $K(\eta)$ that have been discussed thus far are shown for comparison in Fig. 3 along with the indicator function. It is noted that the bias for the Split-Bernstein function K_{SB} and the indicator function are both zero due to the design of the functions.

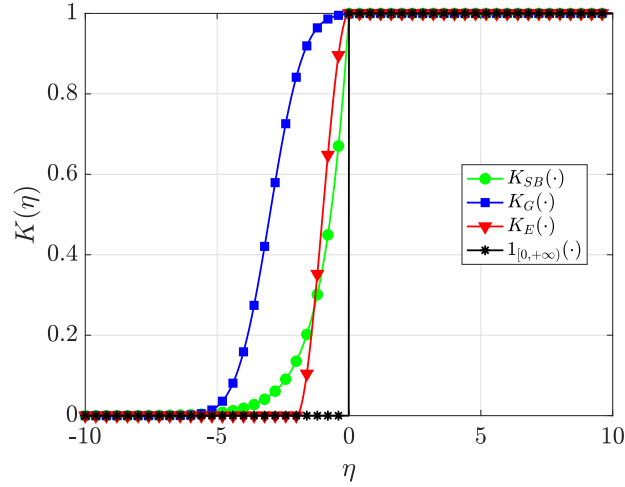


Figure 3: Biased kernel function $K(\cdot)$ and the indicator function.

The new method of biased KDEs that leads to a nonlinear approximation of the chance constraint that provides an upper bound on the chance constraint has been derived. This method can be applied to transform chance constrained optimization problems to deterministic optimization problems, particularly chance constrained optimal control problems.

3 Chance Constrained Optimal Control

Consider the following continuous time CCOC. Determine the state $\mathbf{y}(\tau) \in \mathbb{R}^{n_y}$ and the control $\mathbf{u}(\tau) \in \mathbb{R}^{n_u}$ on the domain $\tau \in [-1, +1]$, the initial time, t_0 , and the terminal time t_f that minimize the cost functional

$$\mathcal{J} = \mathcal{M}(\mathbf{y}(-1), t_0, \mathbf{y}(+1), t_f) + \frac{t_f - t_0}{2} \int_{-1}^{+1} \mathcal{L}(\mathbf{y}(\tau), \mathbf{u}(\tau), t(\tau, t_0, t_f)) d\tau, \quad (52a)$$

subject to the dynamic constraints

$$\frac{d\mathbf{y}}{d\tau} - \frac{t_f - t_0}{2} \mathbf{a}(\mathbf{y}(\tau), \mathbf{u}(\tau), t(\tau, t_0, t_f)) = \mathbf{0}, \quad (52b)$$

the inequality path constraints

$$\mathbf{c}_{\min} \leq \mathbf{c}(\mathbf{y}(\tau), \mathbf{u}(\tau), t(\tau, t_0, t_f)) \leq \mathbf{c}_{\max}, \quad (52c)$$

the boundary conditions

$$\mathbf{b}_{\min} \leq \mathbf{b}(\mathbf{y}(-1), t_0, \mathbf{y}(+1), t_f) \leq \mathbf{b}_{\max}, \quad (52d)$$

and the chance-constraints

$$P(\mathbf{F}(\mathbf{y}(\tau), \mathbf{u}(\tau), t(\tau, t_0, t_f)); \boldsymbol{\xi}) \leq \mathbf{q}) \geq 1 - \epsilon. \quad (52e)$$

It is noted that the time interval $\tau \in [-1, +1]$ can be transformed to the time interval $t \in [t_0, t_f]$ via the affine transformation

$$t \equiv t(\tau, t_0, t_f) = \frac{t_f - t_0}{2} \tau + \frac{t_f + t_0}{2}. \quad (53)$$

where \mathbf{y} is the state defined on the feasible set $\mathbf{Y} \subset \mathbb{R}^n$. The control \mathbf{u} is defined on the feasible set $\mathbf{U} \subset \mathbb{R}^m$. The parameters and variables related to the chance constraint were described in Section 2.2. It should be noted that a chance constraint can be used to represent both path, dynamic and event probabilistic constraints.

Before applying the method of biased KDEs to CCOCs to transform the chance constraints to nonlinear constraint approximations, the continuous time CCOC must be transformed to a form that can be solved using numerical methods. For application with numerical methods, the CCOC is discretized on the domain $\tau \in [-1, +1]$ which is partitioned into a *mesh* consisting of K *mesh intervals* $\mathcal{S}_k = [T_{k-1}, T_k]$, $k = 1, \dots, K$, where $-1 = T_0 < T_1 < \dots < T_K = +1$. The mesh intervals have the property that $\cup_{k=1}^K \mathcal{S}_k = [-1, +1]$. Let $\mathbf{y}^{(k)}(\tau)$ and $\mathbf{u}^{(k)}(\tau)$ be the state and control in \mathcal{S}_k . Using the transformation given in Eq. (53), the chance constrained optimal control problem of Eqs. (52a)-(52e) can then be rewritten as follows. Minimize the cost functional

$$\mathcal{J} = \mathcal{M}(\mathbf{y}^{(1)}(-1), t_0, \mathbf{y}^{(K)}(+1), t_f) + \frac{t_f - t_0}{2} \sum_{k=1}^K \int_{T_{k-1}}^{T_k} \mathcal{L}(\mathbf{y}^{(k)}(\tau), \mathbf{u}^{(k)}(\tau), t) d\tau, \quad (54a)$$

subject to the dynamic constraints

$$\frac{d\mathbf{y}^{(k)}(\tau)}{d\tau} - \frac{t_f - t_0}{2} \mathbf{a}(\mathbf{y}^{(k)}(\tau), \mathbf{u}^{(k)}(\tau), t) = \mathbf{0}, \quad (k = 1, \dots, K), \quad (54b)$$

the path constraints

$$\mathbf{c}_{\min} \leq \mathbf{c}(\mathbf{y}^{(k)}(\tau), \mathbf{u}^{(k)}(\tau), t) \leq \mathbf{c}_{\max}, \quad (k = 1, \dots, K), \quad (54c)$$

the boundary conditions

$$\mathbf{b}_{\min} \leq \mathbf{b}(\mathbf{y}^{(1)}(-1), t_0, \mathbf{y}^{(K)}(+1), t_f) \leq \mathbf{b}_{\max}, \quad (54d)$$

and the chance-constraints

$$P(\mathbf{F}(\mathbf{y}^{(k)}(\tau), \mathbf{u}^{(k)}(\tau), t; \boldsymbol{\xi}) \leq \mathbf{q}) \geq 1 - \epsilon. \quad (54e)$$

Because the state must be continuous at each interior mesh point, it is required that the condition $\mathbf{y}(T_k^-) = \mathbf{y}(T_k^+)$, $(k = 1, \dots, K - 1)$ be satisfied at the interior mesh points (T_1, \dots, T_{K-1}) .

4 Legendre-Gauss-Radau Collocation

The form of discretization that will be applied to the CCOCP in Section 3 is collocation at Legendre-Gauss-Radau (LGR) points [31, 32, 33]. In the LGR collocation method, the state of the continuous-time CCOCP is approximated in \mathcal{S}_k , $k \in [1, \dots, K]$, as

$$\begin{aligned} \mathbf{y}^{(k)}(\tau) &\approx \mathbf{Y}^{(k)}(\tau) = \sum_{j=1}^{N_k+1} \mathbf{Y}_j^{(k)} \ell_j^{(k)}(\tau), \\ \ell_j^{(k)}(\tau) &= \prod_{\substack{l=1 \\ l \neq j}}^{N_k+1} \frac{\tau - \tau_l^{(k)}}{\tau_j^{(k)} - \tau_l^{(k)}}, \end{aligned} \quad (55)$$

where $\tau \in [-1, +1]$, $\ell_j^{(k)}(\tau)$, $j = 1, \dots, N_k + 1$, is a basis of Lagrange polynomials, $(\tau_1^{(k)}, \dots, \tau_{N_k}^{(k)})$ are the Legendre-Gauss-Radau (LGR) [31] collocation points in $\mathcal{S}_k = [T_{k-1}, T_k)$, and $\tau_{N_k+1}^{(k)} = T_k$ is a noncollocated point. Differentiating $\mathbf{Y}^{(k)}(\tau)$ in Eq. (55) with respect to τ gives

$$\frac{d\mathbf{Y}^{(k)}(\tau)}{d\tau} = \sum_{j=1}^{N_k+1} \mathbf{Y}_j^{(k)} \frac{d\ell_j^{(k)}(\tau)}{d\tau}. \quad (56)$$

Defining $t_i^{(k)} = t(\tau_i^{(k)}, t_0, t_f)$ using Eq. (53), the dynamics are then approximated at the N_k LGR points in mesh interval $k \in [1, \dots, K]$ as

$$\sum_{j=1}^{N_k+1} D_{ij}^{(k)} \mathbf{Y}_j^{(k)} - \frac{t_f - t_0}{2} \mathbf{a}(\mathbf{Y}_i^{(k)}, \mathbf{U}_i^{(k)}, t_i^{(k)}) = \mathbf{0}, \quad (i = 1, \dots, N_k), \quad (57)$$

where $D_{ij}^{(k)} = d\ell_j^{(k)}(\tau_i^{(k)})/d\tau$, ($i = 1, \dots, N_k$), ($j = 1, \dots, N_k + 1$) are the elements of the $N_k \times (N_k + 1)$ *Legendre-Gauss-Radau differentiation matrix* [31] in mesh interval \mathcal{S}_k , $k \in [1, \dots, K]$. The LGR discretization then leads to the following nonlinear programming problem (NLP). Minimize

$$\mathcal{J} \approx \mathcal{M}(\mathbf{Y}_1^{(1)}, t_0, \mathbf{Y}_{N_K+1}^{(K)}, t_f) + \sum_{k=1}^K \sum_{j=1}^{N_k} \frac{t_f - t_0}{2} w_j^{(k)} \mathcal{L}(\mathbf{Y}_j^{(k)}, \mathbf{U}_j^{(k)}, t_j^{(k)}), \quad (58)$$

subject to the collocation constraints of Eq. (57) and the constraints

$$\mathbf{c}_{\min} \leq \mathbf{c}(\mathbf{Y}_i^{(k)}, \mathbf{U}_i^{(k)}, t_i^{(k)}) \leq \mathbf{c}_{\max}, \quad (i = 1, \dots, N_k), \quad (59)$$

$$\mathbf{b}_{\min} \leq \mathbf{b}(\mathbf{Y}_1^{(1)}, t_0, \mathbf{Y}_{N_K+1}^{(K)}, t_f) \leq \mathbf{b}_{\max}, \quad (60)$$

$$P(\mathbf{F}(\mathbf{Y}_i^{(k)}, \mathbf{U}_i^{(k)}, t_i^{(k)}; \boldsymbol{\xi}) \leq \mathbf{q}) \geq 1 - \epsilon, \quad (i = 1, \dots, N_k), \quad (61)$$

$$\mathbf{Y}_{N_k+1}^{(k)} = \mathbf{Y}_1^{(k+1)}, \quad (k = 1, \dots, K - 1), \quad (62)$$

where $N = \sum_{k=1}^K N_k$ is the total number of LGR points and Eq. (62) is the continuity condition on the state and is enforced at the interior mesh points (T_1, \dots, T_{K-1}) by treating $\mathbf{Y}_{N_k+1}^{(k)}$ and $\mathbf{Y}_1^{(k+1)}$ as the same variable in the NLP.

As the CCOCP is now in a discretized form, the method of biased KDEs developed in Section 2 can be applied to transform the discretized CCOCP to a discretized deterministic optimal control problem. The deterministic optimal control problem resulting from the application of LGR collocation and the method of biased KDEs to the continuous-time CCOCP can now be solved using available software.

5 Biased Kernel Method for Chance Constraints

In this section, a computational framework to solve CCOCPs in their deterministic optimal control problem form is described that combines the theory of Sections 2, 3 and 4. Such a framework can be computationally expensive due to the evaluation of the chance constraint approximation at each collocation point for 50,000+ MCMC samples. For certain CCOCPs, a larger bandwidth can first be applied to obtain an over-smooth constraint approximation that can lead to faster convergence of the NLP. When the NLP solver is in the neighborhood of the solution, the bandwidth can then be decreased to reach a less conservative solution. The computational implementation of Sections 2, 3, and 4 is presented below as the Method of Biased Kernels for Chance Constrained Optimal Control.

Method of Biased Kernels for Chance Constrained Optimal Control

Step 1: Reformulate chance constraint to transform CCOCP to deterministic optimal control problem using the method of Section 2.3.

Step 2: Obtain MCMC samples of random variables.

Step 3: Choose a bandwidth h .

(a): Determine a trial h_i value.

(b): Run optimal control problem through optimal control software for up to four mesh refinement iterations.

(c): If NLP has converged and error tolerance for mesh is within ϵ , set $h = h_i$, otherwise choose $h_{i+1} > h_i$ and return to **3b**.

Step 4: Set bandwidth as $h > h_i$ if error tolerance decreases to ϵ in less iterations, based on **Step 3**, otherwise continue to **Step 5**.

Step 5: Run optimal control problem through optimal control software with mesh refinement and possible switch of h to h_i .

Step 6: Return to **Step 5** to repeat 20+ times to ensure of NLP convergence for each run.

6 Application of Method

In this section, the computational framework described in Section 5 is applied to an example. The example is a chance constrained soft lunar landing optimal control problem from Ref. [22] that is a modification of the deterministic soft lunar landing optimal control problem from Ref. [42]. The example is used to compare the application of the method of biased KDEs with three different kernels to results already available in the literature [22] for a CCOCP with a control dependent path chance constraint and an event chance constraint.

The three kernels chosen for comparison were the Split-Bernstein, Epanechnikov, and Gaussian kernels.

Each kernel was chosen based on different properties of the integrated function $K(\cdot)$. The Split-Bernstein function $K_{SB}(\cdot)$ tightly bounds the indicator function due to its left biased exponential form. The Epanechnikov function $K_E(\cdot)$ does not provide as tight a bound, but it is a smoother function than the Split-Bernstein function K_{SB} and was proven in Section 2.3.2 to satisfy the requirement of **Theorem 1** with the correct choice of bias. The Epanechnikov function K_E is a piecewise function like the Split-Bernstein function K_{SB} . Thus the application of either kernel to available optimal control software could result in an increase in computational expense as opposed to a completely smooth kernel. As a result, the Gaussian kernel was also included for comparison due to the smoothness of the function K_G , despite not having a bias that satisfies of the requirement of **Theorem 1** as discussed in Section 2.3.

The example was solved in MATLAB[®] version R2018a (build 9.4.0.813654) using the optimal control software package GPOPS – III [43] together with the NLP solver SNOPT [36, 44]. GPOPS – III implements an hp-adaptive LGR collocation method [31, 32, 45, 33, 46, 47, 48, 49, 50]. Derivative approximations required by SNOPT were obtained using central finite-differencing [51]. Additionally, the NLP solver tolerance and maximum number of iterations were set to 10^{-6} and 500, respectively. Mesh refinement was performed using the method of Ref. [47] with a mesh refinement accuracy tolerance of 10^{-6} and decay rate of 0.5 (as required by the method of Ref. [47]). The initial mesh consisted of 10 mesh intervals with four collocation points each. A Hamiltonian Monte Carlo (HMC) method was chosen to obtain the 50,000 MCMC samples as described in Neal [52, 53] that were generated for each run. The bandwidths were determined using the MATLAB[®] function *ksdensity* that employs methods from Refs. [54, 55]. Twenty runs for each kernel were performed using a 2.9 GHz Intel[®] Core i9 Macbook Pro running Mac OS-X version 10.13.6 (High Sierra) with 32 GB 2400 MHz DDR4 RAM. The times recorded in this paper are the times for each run.

6.1 Soft Lunar Landing Optimal Control Problem

Consider the following chance constrained modification of the soft lunar landing optimal control problem.

Minimize the cost functional

$$\min J = \int_0^{t_f} u dt, \quad (63)$$

subject to the dynamic constraints

$$\begin{aligned}\dot{y}_1(t) &= y_2(t), \\ \dot{y}_2(t) &= g + u(t),\end{aligned}\tag{64}$$

the boundary conditions

$$\begin{aligned}y_1(0) &= 10, \quad y_1(t_f) = \textit{free}, \\ y_2(0) &= -2, \quad y_2(t_f) = 0,\end{aligned}\tag{65}$$

the control bounds

$$u \geq 0,\tag{66}$$

the chance event constraint

$$\epsilon_a \geq P(|y_1(t_f) - \xi_1| - \delta > 0),\tag{67}$$

and the chance path constraint

$$\epsilon_b \geq P(u + \xi_2 - 3 > 0),\tag{68}$$

where $g = 1.622$ and $\delta = 0.250$. The risk violation parameters were set as $\epsilon_a = 0.1$ and $\epsilon_b = 0.01$. The random variable ξ_1 was assigned a distribution of the form $N(0, 0.1^2)$, while the random variable ξ_2 was assigned the following bimodal distribution:

$$\xi_2 \sim \frac{1.03}{0.05\sqrt{2\pi}} \exp\left(\frac{-x^2}{2(0.05^2)}\right) + \frac{1.12}{0.08\sqrt{2\pi}} \exp\left(\frac{-(x+0.07)^2}{(0.08^2)}\right).\tag{69}$$

The initial guess was a straight line approximation between the known initial and terminal conditions. If endpoint conditions were not available, a constant initial guess that did not violate the constraint bounds was used. The control was set as a constant of zero for the initial guess.

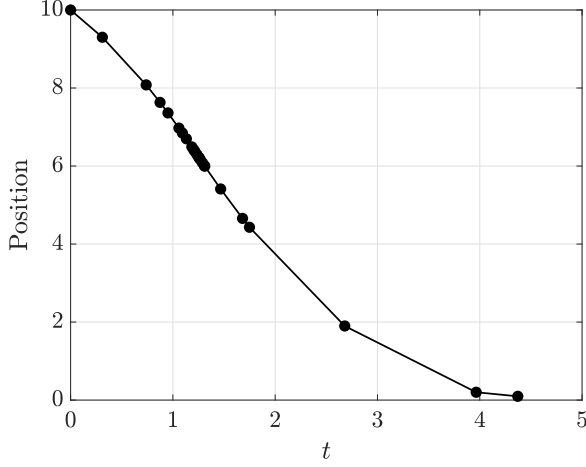
In order to better compare results, the solution to the following deterministic soft lunar landing optimal control problem was also computed. Minimize Eq. (63), subject to the dynamic constraints of Eq.(64), the boundary conditions

$$\begin{aligned}y_1(0) &= 10, \quad y_1(t_f) = 0, \\ y_2(0) &= -2, \quad y_2(t_f) = 0,\end{aligned}\tag{70}$$

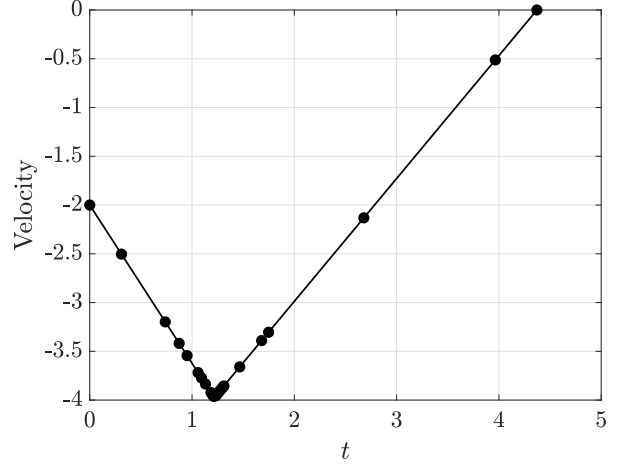
and the control bounds

$$0 \leq u \leq 3.\tag{71}$$

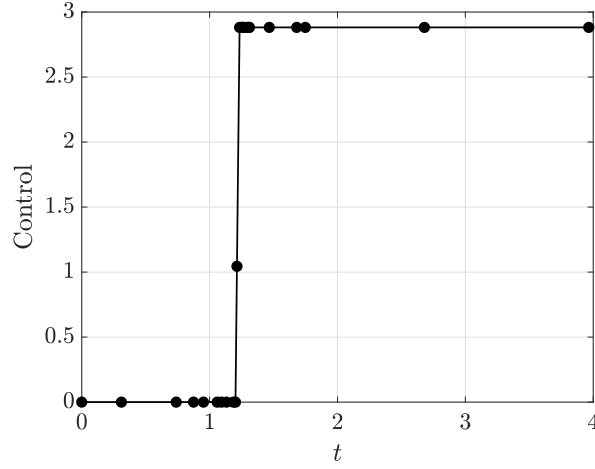
As mentioned in Section 5, evaluation of the chance constraint at each collocation point can be computationally expensive because of the large number of MCMC samples. In order to reduce the computation time



(a) Example problem position.



(b) Example problem velocity.



(c) Example problem control.

Figure 4: Example results using Split-Bernstein kernel.

required to solve the NLP, the chance constraint of Eq. (68) was replaced by the following chance constraint:

$$\epsilon_b \geq \begin{cases} 0, & \text{if } u \leq 3 - b, \\ P(u + \xi_2 - 3 > 0), & \text{if } u > 3 - b, \end{cases} \quad (72)$$

where $b = 1$. The reformulated chance constraint of Eq. (72) does not change the solution if b is properly chosen. In particular, looking at the form of the chance constraint in Eq. (68), unless the control is close to its maximum the chance constraint will evaluate to a small number. Consequently, implementation of the path chance constraint of Eq. (72) prevents the NLP solver from unnecessarily evaluating 50,000+ MCMC samples at every collocation point.

The solution obtained for one run applying the Split-Bernstein kernel is shown in Fig. 4, where it is noted that all three kernels have similar solutions and thus only one figure is included for reference. The control still maintains the bang-bang structure of the solution to the deterministic optimal control problem with a lower maximum control than that of the solution to the deterministic optimal control, in order to satisfy the path chance constraint. Additionally, all three kernels satisfy the event constraint as the average final positions for the Split-Bernstein, Gaussian, and Epanechnikov kernels are, respectively, 0.1100, 0.1100, and 0.1111.

Table 1: Run results for Example

	Gaussian	Split-Bernstein	Epanechnikov	Deterministic
μ_{J^*}	9.1375	9.0934	9.0909	8.9069
σ_{J^*}	0.0042	0.0034	0.0031	0
μ_T	3.2567 s	4.0141 s	5.9531 s	0.1109 s
σ_T	1.1129 s	0.8698 s	1.6313 s	0.02039 s
T_{\max}	5.9796 s	6.3566 s	10.4826 s	0.2073 s
T_{\min}	1.8637 s	3.1013 s	3.6148 s	0.0979 s

Table 1 compares the results obtained using the algorithm outlined in Section 5 for twenty runs of the chance constrained version of the example applying each of the three kernels, alongside the results obtained for the deterministic formulation of the example. In Table 1, J^* is the optimal cost and T is the total time for a call to the optimal control software to reach convergence for one run, where the time T does not include the time to generate the initial setup for each run. For the results shown in Table 1, the bandwidths for the path and event chance constraints were initially set to 0.01 and 0.02, respectively, for the Gaussian kernel and were set to 0.02 and 0.03, respectively, for the other two kernels. Applying the criteria provided in the algorithm in Section 5, the bandwidths were switched to the bandwidths determined using *ksdensity* for the path and event chance constraints as approximately 0.008 and 0.01, respectively, for all three kernels. The results shown in Table 1 compare well with the results obtained using the Split-Bernstein approximation method from Ref. [22]. The average optimal costs obtained using the three kernels are larger than the

optimal cost from Ref. [22]. This discrepancy in optimal cost is due to the application of the automated bandwidth selection method resulting in bandwidths that were different for each constraint, as well as being larger than the bandwidth applied for both constraints in Ref. [22]. The automated bandwidth selection method determined those bandwidths that most effectively balanced the trade-off between the error and variance of the biased KDE applied to each constraint.

Next, comparing the results for the three kernels from Table 1, the Gaussian kernel had a lower run time than the other two kernels, as expected due to the smoothness of the function K_G . The Epanechnikov kernel had the worst average run time, due to more internal operations being required when applying this kernel. The average optimal costs between the three kernels do not vary significantly, with the average optimal cost for the Epanechnikov kernel being the smallest. The average optimal cost for the Gaussian kernel was the largest as a result of this kernel having a larger bias than those of the other kernels. Moreover, the run times for solving both the chance constrained and deterministic formulations of the example are small enough to be considered computationally efficient. Finally, while the average optimal costs are higher than the deterministic optimal cost, the differences are small.

7 Conclusions

A method has been developed for approximating chance constraints as nonlinear constraints using biased KDEs with MCMC sampling to transform CCOCs to deterministic optimal control problems. This method combines the advantages of previous method for reformulating the chance constraints as the biased KDEs not only provide an upper bound on the chance constraint, but are also approximate CDFs. The method of biased KDEs was then applied to an example for three different kernels. Two of the kernels chosen, the Split-Bernstein and Epanechnikov kernels, were chosen as they satisfied the necessary requirements to obtain the correct form of a biased KDE. The third kernel chosen was the Gaussian kernel (added for the smoothness of its integrated function), despite not meeting the qualifications to obtain the correct form of a biased KDE. The Gaussian kernel had the lowest average computation time among the kernels, indicating that smoothness affects computational efficiency. The Epanechnikov kernel had the lowest average optimal cost, which was still higher than the optimal cost for a deterministic formulation of the example. Transforming CCOCs

to deterministic optimal control problems using the method of biased KDEs with MCMC sampling shows promise as the resulting optimal control problem can be solved using available optimal control software. With fine tuning, the computational performance of this method could be made comparable to results obtained using a conservative deterministic formulation of the same CCOCP.

8 Acknowledgments

The authors gratefully acknowledge support for this research from the from the U.S. National Science Foundation under grants CMMI-1563225, DMS-1522629, and DMS-1819002.

References

- [1] Betts, J. T., *Practical Methods for Optimal Control and Estimation Using Nonlinear Programming*, SIAM Press, Philadelphia, 2nd ed., 2009.
- [2] Yan, J. and Bitmead, R. R., “Incorporating State Estimation into Model Predictive Control and Its Application to Network Traffic Control,” *Automatica*, Vol. 41, No. 4, April 2005, pp. 595–604.
- [3] Li, P., Arellano-Garcia, H., and Wozny, G., “Chance Constrained Programming Approach to Process Optimization under Uncertainty,” *Computers & Chemical Engineering*, Vol. 32, No. 1-2, Jan. 2008, pp. 25–45.
- [4] Li, P., Wendt, M., and Wozny, G., “A Probabilistically Constrained Model Predictive Controller,” *Automatica*, Vol. 38, No. 7, July 2002, pp. 1171–1176.
- [5] Farina, M., Giulioni, L., Magni, L., and Scattolini, R., “A probabilistic approach to model predictive control,” *IEEE Conference on Decision and Control*, December 2013, pp. 7734–7739.
- [6] Keil, R., Aggarwal, R., Kumar, M., and Rao, A. V., “Application of Chance-Constrained Optimal Control to Optimal Obstacle Avoidance,” *AIAA Guidance, Navigation and Control Conference, San Diego*, January 2019, pp. DOI: 10.2514/6.2019-0647.
- [7] Geletu, A., Kloppel, M., Zhang, H., and Li, P., “Advances and applications of chance-constrained approaches to systems optimisation under uncertainty,” *International Journal of Systems Science*, Vol. 44, No. 7, 2013, pp. 1209–1232.
- [8] Blackmore, L., Ono, M., Bektasov, A., and Williams, B. C., “A Probabilistic Particle-Control Approximation of Chance-Constrained Stochastic Predictive Control,” *IEEE Transactions on Robotics*, Vol. 26, No. 3, June 2010, pp. 502–517.
- [9] Blackmore, L., Ono, M., and Williams, B. C., “Chance-Constrained Optimal Path Planning With Obstacles,” *IEEE Transactions on Robotics*, Vol. 27, No. 6, December 2011, pp. 1080–1094.
- [10] Ono, M., Blackmore, L., and Williams, B. C., “Chance Constrained Finite Horizon Optimal Control with Nonconvex Constraints,” *Proceedings of the 2010 American Control Conference*, IEEE, Baltimore, MD, 2010, pp. 1145–1152.
- [11] Okamoto, K. and Tsiotras, P., “Optimal Stochastic Vehicle Path Planning Using Covariance Steering,” *IEEE Robotics and Automation Letters*, Vol. 4, No. 3, July 2019, pp. 2276–2281.
- [12] Hokayem, P., D. Chatterjee, D., and Lygeros, J., “Chance-constrained LQG with bounded control policies,” *IEEE Conference on Decision and Control*, Florence, Italy, December 2013, p. 2471–2476.

- [13] Muhlpfordt, T., Faulwasser, T., and Hagenmeyer, V., “A generalized framework for chance-constrained optimal power flow,” *Sustainable Energy, Grids and Networks*, Vol. 16, 2018, pp. 231–242.
- [14] Pintér, J., “Deterministic Approximations of Probability Inequalities,” *Zeitschrift für Operations Research*, Vol. 33, No. 4, July 1989, pp. 219–239.
- [15] Nemirovski, A. and Shapiro, A., “Convex Approximations of Chance Constrained Programs,” *SIAM Journal on Optimization*, Vol. 17, No. 4, November 2006, pp. 969–996.
- [16] Pagnoncelli, B. K., Ahmed, S., and Shapiro, A., “Sample Average Approximation Method for Chance Constrained Programming: Theory and Applications,” *Journal of Optimization Theory and Application*, Vol. 142, 2009, pp. 399–416. <https://doi.org/10.1007/s10957--009--9523--6>.
- [17] Ono, M., Pavone, M., Kuwata, Y., and Balaram, J., “Chance-Constrained Dynamic Programming with Application to Risk-Aware Robotic Space Exploration,” *Autonomous Robots*, Vol. 39, No. 4, Dec. 2015, pp. 555–571.
- [18] Calafiore, G. C. and Campi, M. C., “The Scenario Approach to Robust Control Design,” *IEEE Transactions on Automatic Control*, Vol. 51, No. 5, May 2006, pp. 742–753.
- [19] Calafiore, G. C. and Fagiano, L., “Robust Model Predictive Control via Scenario Optimization,” *IEEE Transactions on Automatic Control*, Vol. 58, No. 1, January 2013, pp. 219–224.
- [20] Campi, M. C. and Garatti, S. A., “A Sampling-and-Discarding Approach to Chance-Constrained Optimization: Feasibility and Optimality,” *Journal of Optimization Theory and Applications*, Vol. 148, 2011, pp. 257–280, DOI: 10.1007/s10957-010-9754-6.
- [21] Chai, R., Savvaris, A., Tsuordos, A., Chai, S., Xia, Y., and Wang, S., “Solving Trajectory Optimization Problems in the Presence of Probabilistic Constraints,” *IEEE Transactions on Cybernetics (Early Access)*, February 2019, pp. DOI: 10.1109/TYCB.2019.2895305.
- [22] Zhao, Z. and Kumar, M., “Split-Bernstein Approach to Chance-Constrained Optimal Control,” *Journal of Guidance, Control, and Dynamics*, Vol. 40, No. 11, November 2017, pp. 2782–2795.
- [23] Ahmed, S., “Convex relaxations of chance constrained optimization problems,” *Optimization Letters*, Vol. 8, No. 1, January 2014, pp. 1–12. DOI:10.1007/s11590-013-0624-7.
- [24] Gopalakrishnan, B., Singh, A. K., Krishna, K. M., and Manocha, D., “Solving Chance Constrained Optimization under Non-Parametric Uncertainty Through Hilbert Space Embedding,” *arXiv*, November 2018, pp. <https://arxiv.org/abs/1811.09311>.
- [25] Calfa, B. A., Grossman, I. E., Agarwal, A., Bury, S. J., and Wassick, J. M., “Data-driven individual and joint chance-constrained optimization via kernel smoothing,” *Computers and Chemical Engineering*, Vol. 78, July 2015, pp. 51–695.
- [26] Caillaud, J.-B., Cerf, M., Sassi, A., Trelat, E., and Zidani, H., “Solving chance constrained optimal control problems in aerospace via Kernel Density Estimation,” *Optimal Control Applications and Methods*, Vol. 39, No. 5, September/October 2018, pp. 1833–1858. DOI: 10.1002/oca.2445.
- [27] von Stryk, O. and Bulirsch, R., “Direct and Indirect Methods for Trajectory Optimization,” *Annals of Operations Research*, Vol. 37, 1992, pp. 357–373.
- [28] Benson, D. A., Huntington, G. T., Thorvaldsen, T. P., and Rao, A. V., “Direct Trajectory Optimization and Costate Estimation via an Orthogonal Collocation Method,” *Journal of Guidance, Control, and Dynamics*, Vol. 29, No. 6, November-December 2006, pp. 1435–1440. <https://doi.org/10.2514/1.20478>.
- [29] Rao, A. V., Benson, D. A., Darby, C. L., Francolin, C., Patterson, M. A., Sanders, I., and Huntington, G. T., “Algorithm 902: GPOPS, A MATLAB Software for Solving Multiple-Phase Optimal Control Problems Using the Gauss Pseudospectral Method,” *ACM Transactions on Mathematical Software*, Vol. 37, No. 2, April–June 2010, Article 22, 39 pages. <https://doi.org/10.1145/1731022.1731032>.

- [30] Elnagar, G., Kazemi, M., and Razzaghi, M., “The Pseudospectral Legendre Method for Discretizing Optimal Control Problems,” *IEEE Transactions on Automatic Control*, Vol. 40, No. 10, 1995, pp. 1793–1796. <https://doi.org/10.1109/9.467672>.
- [31] Garg, D., Patterson, M. A., Darby, C. L., Francolin, C., Huntington, G. T., Hager, W. W., and Rao, A. V., “Direct Trajectory Optimization and Costate Estimation of Finite-Horizon and Infinite-Horizon Optimal Control Problems via a Radau Pseudospectral Method,” *Computational Optimization and Applications*, Vol. 49, No. 2, June 2011, pp. 335–358. DOI: 10.1007/s10589-00-09291-0.
- [32] Garg, D., Patterson, M. A., Hager, W. W., Rao, A. V., Benson, D. A., and Huntington, G. T., “A Unified Framework for the Numerical Solution of Optimal Control Problems Using Pseudospectral Methods,” *Automatica*, Vol. 46, No. 11, November 2010, pp. 1843–1851. <https://doi.org/10.1016/j.automatica.2010.06.048>.
- [33] Patterson, M. A., Hager, W. W., and Rao, A. V., “A *ph* Mesh Refinement Method for Optimal Control,” *Optimal Control Applications and Methods*, Vol. 36, No. 4, July–August 2015, pp. 398–421. <https://doi.org/10.1002/oca.2114>.
- [34] Canuto, C., Hussaini, M. Y., Quarteroni, A., and Zang, T. A., *Spectral Methods in Fluid Dynamics*, Springer-Verlag, Heidelberg, Germany, 1988.
- [35] Fornberg, B., *A Practical Guide to Pseudospectral Methods*, Cambridge University Press, New York, 1998.
- [36] Gill, P. E., Murray, W., and Saunders, M. A., “SNOPT: An SQP Algorithm for Large-Scale Constrained Optimization,” *SIAM Review*, Vol. 47, No. 1, January 2002, pp. 99–131. <https://doi.org/10.1137/S0036144504446096>.
- [37] Biegler, L. T., Ghattas, O., Heinkenschloss, M., and van Bloemen Waanders, B., editors, *Large-Scale PDE Constrained Optimization*, Lecture Notes in Computational Science and Engineering, Vol. 30, Springer-Verlag, Berlin, 2003.
- [38] Hwang, J.-N., Lay, S.-R., and Lippman, A., “Nonparametric Multivariate Density Estimation: A Comparative Study,” *IEEE Transactions on Signal Processing*, Vol. 42, No. 10, October 1994, pp. 2795 – 2810.
- [39] Anurag and Paragios, N., “Motion-Based Background Subtraction using Adaptive Kernel Density Estimation,” *Proceedings of the 2004 IEEE Computer Society Conference on Computer Vision and Pattern Recognition, IEEE*, June/July 2004, pp. DOI: 10.1109/CVPR.2004.1315179.
- [40] Hodges Jr., J. L. and Lehmann, E. L., “The Efficiency of Some Nonparametric Competitors of the t-Test,” *The Annals of Mathematical Statistics*, Vol. 27, No. 2, June 1956, pp. 324 – 335.
- [41] Epanechnikov, V. A., “Nonparametric Estimation of a Multivariate Probability Density,” *Teor. Veroyatnost. i Primenen*, Vol. 14, No. 1, 1969, pp. 156–161.
- [42] Meditch, J., “On the Problem of Optimal Thrust Programming for a Soft Lunar Landing,” *IEEE Transaction on Automatic Control*, Vol. 9, No. 4, October 1964, pp. 477–484. <https://doi.org/10.1109/TAC.1964.1105758>.
- [43] Patterson, M. A. and Rao, A. V., “GPOPS – III, A MATLAB Software for Solving Multiple-Phase Optimal Control Problems Using *hp*-Adaptive Gaussian Quadrature Collocation Methods and Sparse Nonlinear Programming,” *ACM Transactions on Mathematical Software*, Vol. 41, No. 1, October 2014, pp. 1:1–1:37. <https://doi.org/10.1145/2558904>.
- [44] Gill, P. E., Murray, W., and Saunders, M. A., *User’s Guide for SNOPT Version 7: Software for Large Scale Nonlinear Programming*, February 2006.
- [45] Garg, D., Hager, W. W., and Rao, A. V., “Pseudospectral Methods for Solving Infinite-Horizon Optimal Control Problems,” *Automatica*, Vol. 47, No. 4, April 2011, pp. 829–837. <https://doi.org/10.1016/j.automatica.2011.01.085>.

- [46] Liu, F., Hager, W. W., and Rao, A. V., “Adaptive Mesh Refinement for Optimal Control Using Non-smoothness Detection and Mesh Size Reduction,” *Journal of the Franklin Institute*, Vol. 352, No. 10, October 2015, pp. 4081–4106. <https://doi.org/10.1016/j.jfranklin.2015.05.028>.
- [47] Liu, F., Hager, W. W., and Rao, A. V., “Adaptive Mesh Refinement for Optimal Control Using Decay Rates of Legendre Polynomial Coefficients,” *IEEE Transactions on Control System Technology*, Vol. 26, No. 4, 2018, pp. 1475 – 1483. <https://doi.org/10.1109/TCST.2017.2702122>.
- [48] Darby, C. L., Hager, W. W., and Rao, A. V., “An *hp*-Adaptive Pseudospectral Method for Solving Optimal Control Problems,” *Optimal Control Applications and Methods*, Vol. 32, No. 4, July–August 2011, pp. 476–502. <https://doi.org/10.1002/oca.957>.
- [49] Darby, C. L., Hager, W. W., and Rao, A. V., “Direct Trajectory Optimization Using a Variable Low-Order Adaptive Pseudospectral Method,” *Journal of Spacecraft and Rockets*, Vol. 48, No. 3, May–June 2011, pp. 433–445. <https://doi.org/10.2514/1.52136>.
- [50] Francolin, C. C., Hager, W. W., and Rao, A. V., “Costate Approximation in Optimal Control Using Integral Gaussian Quadrature Collocation Methods,” *Optimal Control Applications and Methods*, Vol. 36, No. 4, July–August 2015, pp. 381–397. <https://doi.org/10.1002/oca.2112>.
- [51] Patterson, M. A. and Rao, A. V., “Exploiting Sparsity in Direct Collocation Pseudospectral Methods for Solving Continuous-Time Optimal Control Problems,” *Journal of Spacecraft and Rockets*, Vol. 49, No. 2, March–April 2012, pp. 364–377. <https://doi.org/10.2514/1.A32071>.
- [52] Neal, R. M., *Handbook of Markov Chain Monte Carlo*, chap. 5, CRC Press, Boca Raton, Florida, 2011, pp. 113–162.
- [53] Neal, R. M., *Probabilistic Inference Using Markov Chain Monte Carlo Methods*, Department of Computer Science, University of Toronto, September 1993, Technical Report, CRG-TR-93-1.
- [54] Bowman, A. and Azzalini, A., *Applied Smoothing Techniques for Data Analysis: The Kernel Approach with S-Plus Illustrations*, Oxford Statistical Science Series, OUP Oxford, 1997.
- [55] Silverman, B. W., *Density Estimation for Statistics and Data Analysis*, Monographs on Statistics and Applied Probability 26, Chapman and Hall/CRC Press, 1986.